Arch Microbiol (2015) 197:181–195
DOI 10.1007/s00203-014-1036-5

ORIGINAL PAPER

Coordinated rearrangements of assimilatory and storage cell compartments in a nitrogen-starving symbiotic chlorophyte cultivated under high light

Olga Gorelova · Olga Baulina · Alexei Solovchenko · Irina Selyakh · Olga Chivkunova · Larisa Semenova · Pavel Scherbakov · Olga Burakova · Elena Lobakova

Received: 9 June 2014 / Revised: 1 September 2014 / Accepted: 6 September 2014 / Published online: 20 September 2014

Abstract A quantitative micromorphometric study of the cell compartment rearrangements was performed in a symbiotic chlorophyte *Desmodesmus* sp. 3Dp86E-1 grown on nitrogen (N) replete or N-free medium under 480 μmol PAR quanta m^{-2} s^{-1}. The changes in the chloroplast, intraplastidial, and cytoplasmic inclusions induced by high light (HL) and N starvation were similar to those characteristic of free-living chlorophytes. The N-sufficient culture responded to HL by a transient swelling of the thylakoid lumen and a decline in photosynthetic efficiency followed by its recovery. In the N-starving cells, a more rapid expansion and thylakoid swelling occurred along with the irreversible decline in the photosynthetic efficiency. Differential induction of starch grains, oil bodies, and cell wall polysaccharides depending on the stress exposure and type was recorded. Tight relationships between the changes in the assimilatory and storage compartments in the stressed *Desmodesmus* sp. cells were revealed.

Keywords Carbon partitioning · Chlorophyta · Micromorphometry · Stress · Symbiotic microalgae · Ultrastructure

Abbreviations

chl	Chlorophyll
CW	Cell wall
HL	High light
N	Nitrogen
Pg	Plastoglobuli
SG	Starch grains
TAG	Triacylglycerines
OB	Oil bodies

Communicated by Erko Stackebrandt.

O. Gorelova · O. Baulina · A. Solovchenko (✉) · I. Selyakh · O. Chivkunova · L. Semenova · P. Scherbakov · O. Burakova · E. Lobakova
Department of Bioengineering Faculty of Biology, Moscow State University, GSP-1, 119234 Moscow, Russia
e-mail: solovchenko@mail.bio.msu.ru

Introduction

Microalgae subjected to stresses such as high light (HL) and essential nutrient, e.g., nitrogen (N) deprivation and/or low temperature, often continue to photosynthesize. At the same time, utilization of the photosynthates becomes limited since N starvation leads to a cessation of cell division (Cunningham and Maas 1978; García-Ferris et al. 1996; Přibyl et al. 2012), thereby increasing the risk of damage to the microalgal cell, especially on the background of high irradiances (Hüner et al. 2012). To avoid photooxidative damage under N starvation, the photosynthates, which are, under favorable conditions, readily consumed for building of the ultrastructural components of the cells, e.g., thylakoid membranes, are channeled into the biosynthesis of reserve compounds such as carbohydrates (starch) or neutral lipids (mainly triacylglycerol, TAG) (Guschina and Harwood 2009; Li et al. 2011; Msanne et al. 2012; Solovchenko 2012; Fernandes et al. 2013). These stress responses are widely employed for the manipulation of metabolism of mass-cultivated microalgae to obtain the biomass enriched in lipids or carbohydrates (Zachleder and Brányiková 2014).

Ultrastructural studies provide an essential insight into the mechanisms of stress acclimation and carbon partitioning in microalgal cells. As a rule, N-starving microalgal cells exhibit a pronounced increase in storage structures, predominantly starch grains (SG) and oil bodies (OB) in size and number with a simultaneous decline in the photoassimilatory

(plastidial) compartment (García-Ferris et al. 1996; Goodson et al. 2011; Dong et al. 2013; Goncalves et al. 2013; Simionato et al. 2013; Yang et al. 2013). Our previous studies revealed tight relationships between stress-induced changes in the contents of photosynthetic pigments and neutral lipids, the main constituents of cytoplasmic OB (Merzlyak et al. 2007; Solovchenko et al. 2009, 2010, 2011). Moreover, there are indications of the lipid acyl group translocation between membranes and storage TAG (Khozin-Goldberg et al. 2005; Goncalves et al. 2013; Simionato et al. 2013). The attention to stress-induced rearrangements of storage compartments of the cell increased recently since oleaginous microalgae are considered as a promising feedstock for biofuel production and an efficient source of the valuable long-chain polyunsaturated fatty acids for feed, food, and nutraceutical purposes (Skjånes et al. 2013).

A number of studies were devoted to the ultrastructural changes during acclimation to stressful illumination conditions without a nutrient limitation (Topf et al. 1992; Fisher et al. 1998). A significant body of ultrastructural evidence of the effects of N starvation and/or HL on cell organization was obtained for diverse free-living microalgae (Merzlyak et al. 2007; Goncalves et al. 2013; Přibyl et al. 2013). At the same time, symbiotic microalgae represent an interesting model for studies of stress physiology of phototrophic microorganisms and hold promise for biotechnology (Gorelova et al. 2012). In spite of these important implications, the information on symbiotic microalgae ultrastructural changes under stress is much more scarce and limited mainly to zooxanthellae (Berner and Izhaki 1994; Muller-Parker et al. 1996).

The present work aims to elucidate the coordinated changes in the photoassimilatory and storage cell compartments induced by HL- and N-starvation stresses in the cells of a symbiotic *Desmodesmus* sp. 3Dp86E-1 isolated in our laboratory (Gorelova et al. 2009). We tried to dissect, using morphometric analysis, the ultrastructural picture of the acclimation of the microalga to HL and N starvation paying special attention to reorganization of the chloroplast, cell wall (CW), and cytoplasmic OB. Distinct patterns of the allocation of the carbon fixed in excess were found. They were dependent on N availability in the medium. Differential response of the CW layers to N starvation was observed. To the best of our knowledge, this is the first report on quantitative ultrastructural investigation of the acclimation of a symbiotic chlorophyte to combination of HL- and N-starvation stresses.

Materials and methods

Strain and cultivation conditions

A strain of microalgae from the genus *Desmodesmus* (R.Chodat) S.S. An, T. Friedl, and E. Hegewald, *Desmodesmus* sp. 3Dp86E-1 was used in this work (for the sake of brevity, it is referred to below as *Desmodesmus* sp.). The strain 3Dp86E-1 was isolated from the association with the hydroid *Dynamena pumila* Linnaeus sampled in Rugozerskaya Guba at Kandalaksha Bay of White Sea (66° 34′ N, 33° 08′ E) as described by Gorelova et al. (2009, 2012). The microalga was identified as *Desmodesmus* sp. (GenBank accession ## JQ313132, KJ463405) and deposited to the microalgal culture collection of Timiryazev Institute of Plant Physiology (IPPAS) under ID IPPAS S-2014.

The cells were grown in complete or nitrogen-free BG-11 medium (Rippka et al. 1979) in glass columns (6.6 cm internal diameter, 1.5 L volume) under continuous illumination of 480 μmol PAR photons m^{-2} s^{-1} by a white light-emitting diode source as measured with a LiCor 850 quantum sensor (LiCor, United States) in the center of an empty column in a temperature-controlled water bath at 27 °C and constant bubbling with air (300 mL min^{-1}).

The initial cultures were grown in flasks on BG-11 medium at 40 μmol PAR photons m^{-2} s^{-1}. The cultures were kept at the exponential phase by daily dilution with the medium. At the beginning of each experiment, cells were harvested by centrifugation (1,200×*g* for 5 min), washed twice in fresh N-free BG-11 medium, and resuspended in the corresponding (complete or N-free) medium to the initial chl concentration and biomass content of 25 and 0.4 g L^{-1}, respectively. The nitrogen content in the medium was checked during the experiment using the nitrate assay kit (Merck, Darmstadt, Germany, Merckoquant 1.10020.001). Under the specified conditions, at least three independent experiments were carried out for each treatment repeated in duplicate columns. The average values ($n = 6$) and corresponding standard errors are shown unless stated otherwise.

Growth estimation was based on the content of chlorophyll (chl, see below) and dry weight (DW) measurements. DW was determined as follows: 5 mL of samples was deposited on a pre-weighed 25 mm GF/F glass fiber filters (Whatman, Maidstone, UK). The filters were dried in a microwave oven to constant weight.

Electron microscopy and cell morphometric analysis

The microalgae samples for TEM were fixed in 2 % (w/v) glutaraldehyde solution in 0.1 M sodium cacodylate buffer at room temperature for 0.5 h and then postfixed for 4 h in 1 % (w/v) OsO_4 in the same buffer. The samples, after dehydration through graded ethanol series including anhydrous ethanol saturated with uranylacetate, were embedded in araldite. Ultrathin sections were made with an LKB-8800 (LKB, Sweden) ultratome, stained with lead citrate according to Reynolds (1963), and examined under JEM-100B or JEM-1011 (JEOL, Tokyo, Japan) microscopes.

All quantitative morphometric analyses were done on sections through the cell equator or subequator; at least ten samples from each treatment were examined. The organelles and inclusions were counted on the sections; frequencies of the organelles and structures were calculated as total section number percentage of cell sections containing the structure of interest. Linear sizes (CW thickness, OB, and plastoglobuli (Pg) diameter) as well as subcellular structure area were measured on the TEM micrographs of the cell ultrathin sections ($n = 20$) using ImageJ software (NIH, Bethesda MA, USA). The significance of the difference in the means was tested by Student's t test using Origin software (OriginLab, Northampton MA, USA). For the sake of clarity, the area of chloroplast excepting the SG and pyrenoid is referred to below as the 'stroma and thylakoid membranes' (STM).

Pigment extraction and analysis

Cells were pelleted by centrifugation, transferred to a glass–glass homogenizer with a chloroform–methanol (10 mL, 2:1, v/v) mixture, and extracted to remove all pigment. The lipid fraction including chl was separated according to Folch et al. (1957). The chloroform phase was used for further pigment and lipid analysis. Chl *a* and *b* were quantified using absorption coefficients for chloroform (Wellburn 1994).

Fatty acid analysis

After completion of the pigment analysis, the chloroform was evaporated and the lipid residue was dissolved in methanol. Fatty acid methyl esters were prepared by transesterification of the lipids by refluxing for 1.5 h in methanol containing 5 % conc. sulfuric acid (Kates 1986) in the presence of 0.01 % 2,6-di-*tert*.-butyl-4-methylphenol, as an antioxidant and heptadecanoic acid (C17:0) as an internal standard. Methyl esters were extracted with *n*-hexane and immediately used for GC analysis. The fatty acid methyl esters were separated and identified; it was done according to the retention times of standards (Sigma, St. Louis MO, USA) and by characteristic mass spectra obtained with Agilent 7890 gas chromatograph equipped with HP5MS UI capillary column coupled with Agilent 5970 mass-selective detector (Agilent, Santa Clara CA, USA). Helium at a flow rate of 1 mL min^{-1} was used as a carrier gas.

Chlorophyll fluorescence measurements

Induction curves of chl fluorescence were recorded using a Fluorpen FP100s portable pulse-amplitude modulated fluorometer (Photon Systems Instruments, Drasov, Czech Republic) and analyzed as described earlier (Solovchenko et al. 2013b). Non-photochemical quenching (NPQ) was calculated as NPQ = Fm/Fm′−1 (Maxwell and Johnson 2000).

Determination of C and N content in biomass

Carbon and nitrogen content in the biomass was determined using an Vario EL Cube CNS (carbon, nitrogen, sulfur) element analyzer (Elementar, Hanau, Germany) calibrated with a certified acetanilide standard (Elementar) as described by de Morais and Costa (2007).

Results

Biomass accumulation and changes in C/N ratio

The culture of *Desmodesmus* sp. grown in complete BG-11 medium (designated as '+N') displayed a rapid accumulation of biomass and chl (Fig. 1) for the first 9 days of cultivation. Displaying an average growth rate of ca. 0.3 g L^{-1} day^{-1}, the '+N' culture reached the stationary phase at 3.2 g L^{-1} DW by the 17th day (Fig. 1a, closed symbols). The culture initiated in the N-free BG-11 medium (referred to below as '−N') accumulated biomass at a much slower rate (Fig. 1a, open symbols) reaching ca. 1 g L^{-1} by the end of the experiment (17 days of cultivation). As shown by the analytical determination of nitrate in the growth media, the '+N' cultures did not encounter N limitation under our experimental conditions.

Generally, the cells grown in N-free medium retain the characteristic round shape, size, and ultrastructural integrity (Fig. 2). After 2 days of cultivation, the protoplast area on equatorial or subequatorial sections of the cells grown

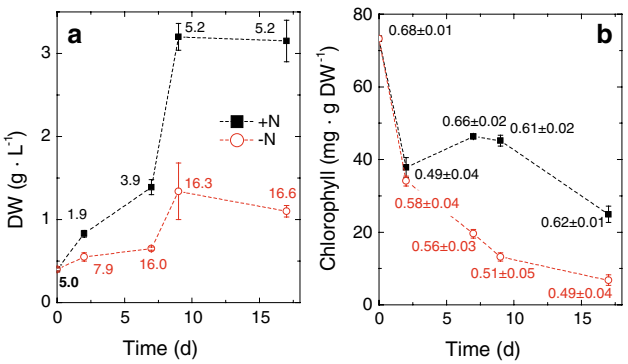

Fig. 1 Growth, C/N ratio, and photosynthetic performance of *Desmodesmus* sp. 3Dp86E-1 in complete and N-free medium. **a** Biomass accumulation. **b** Changes in chlorophyll content per unit DW. Numbers in panel **a**: DW percentages for C and N determined at the corresponding cultivation days. Numbers in **b**: potential maximal quantum yield of the photosystem II (Fv/Fm)

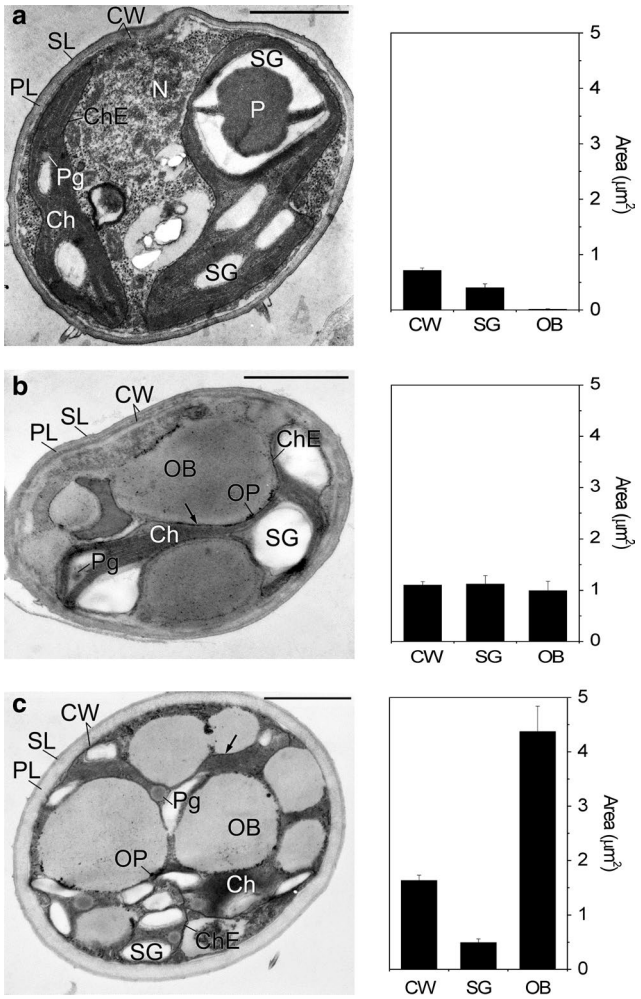

Fig. 2 Ultrastructure of *Desmodesmus* sp. 3Dp86E-1 cells (TEM micrographs) and (histograms) area of the CW and the major storage cell subcompartments. **a** In the inoculum (day 0) and after 17 days of growth in, **b** N-replete or, **c** N-free-medium. *Ch* chloroplast, *ChE* chloroplast envelope, *CW* cell wall, *N* nucleus, *OB* oil body, *OP* osmiophilic particles, *P* pyrenoid, *Pg* plastoglobuli, *PL* polysaccharide layer of CW, *SG* starch grain, *SL* trilaminar sporopollenin layer of CW. *Arrows* point to the contacts between chloroplast envelope and oil body. *Scale bars* 1 μm

in complete and N-free medium comprised, on an average, 12 and 8 μm^2; at more prolonged cultivation times, the size of the '+N' cell protoplast decreased to ca. 6–7 μm^2, whereas in the area of the '−N' cells, it comprised ca. 9 μm^2. Sporangia with autospores were encountered in the '+N' culture throughout the whole cultivation period but more frequently at the exponential phase, suggesting vigorous division of the cells in this culture. In the '−N' culture, sporangia were encountered only during the first week of cultivation and were significantly less frequent.

The '+N' cells possessed stable C and N contents; hence, the C/N ratio remained almost invariable (ca. 5) during the experiment (numbers in Fig. 1a). On the contrary, in the N-deprived cells, C content increased remarkably on the background of the decline of N content; consequently, C/N ratio showed a dramatic rise (from 5 to ca. 18) within the first 7 day of cultivation and remained almost unchanged thereafter.

Changes in chloroplast organization, chlorophyll content, and photosystem II efficiency

Under N starvation, conspicuous changes were recorded in the chloroplast size and organization (Fig. 2). Chloroplast remained the largest organelle of the cell of the *Desmodesmus* sp. albeit its area decreased remarkably (from 3.546 ± 0.224 to 1.645 ± 0.237 and 3.169 ± 0.341 μm^2 in the '−N' and '+N' cells, respectively). The shrinkage of the chloroplast was accompanied by profound alteration of its morphology and ultrastructure. The chloroplast retained its lobed shape. At the same time, its surface area expanded as evidenced by the increase in the perimeter-to-area ratio (3.84 ± 0.37 vs. 9.66 ± 0.49 at the 17th day for '+N' and '−N' cells, respectively). The perimeters of the chloroplasts on cell sections comprised, by the 17th day of cultivation, 10.51 ± 0.96 and 14.84 ± 1.59 μm in N-replete and N-lacking media, respectively. A simultaneous decline in linolenic (18:3) acid characteristic mostly of chloroplast lipids was recorded on the background of the increase in oleate (18:1), a major fatty acid of reserve triacylglycerides (Table 2). As a result, the unsaturation index of the fatty acids of the *Desmodesmus* sp. cell lipids decreased by the 9th day of cultivation from 129.7 to 99.43 and 99.66 in the '+N' and '−N' cells, respectively (Table 2).

Both membranes of the chloroplast envelope retained high osmiophilicity (Figs. 2, 4, 5). The percentage of the stroma and thylakoid membranes of the chloroplast (STM) of total chloroplast or protoplast area declined in the course of cultivation; the rate of the decline was higher in the '−N' cells in comparison with the '+N' cells (squares in Fig. 3). At the same time, the kinetics of the changes in STM area percentage of the total chloroplast area were similar in the '+N' and '−N' cells (triangles in Fig. 3).

As expected for cultivation under HL, a remarkable (ca. two-time) drop in chl content per unit DW occurred in the *Desmodesmus* sp. within the first 2 days regardless of N availability in the medium (Fig. 1b). In the '+N' culture, chl content was recovered slightly by the 9th day and then declined slowly till the end of the experiment. By contrast, no recovery took place in the '−N' cells where chl content declined steadily for the whole cultivation period (17 days).

The initial decline in chl content was accompanied, as revealed by chl fluorescence measurement (numbers in Fig. 1b), by a corresponding decline in the PSII efficiency (Q_y), which was more pronounced in the '+N' culture. Similarly to chl content, Q_y was recovered in the '+N' cells

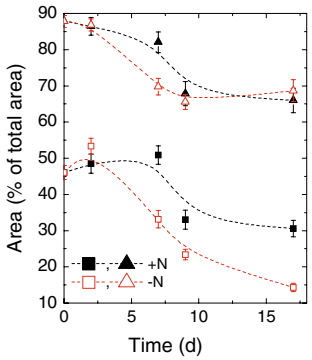

Fig. 3 Changes in the proportion of the stroma and thylakoid membranes of the chloroplast (STM) within the total area of protoplast (*squares*) or chloroplast (*triangles*) of the *Desmodesmus* sp. 3Dp86E-1 cells grown in complete (*closed symbols*) or (*open symbols*) N-free medium

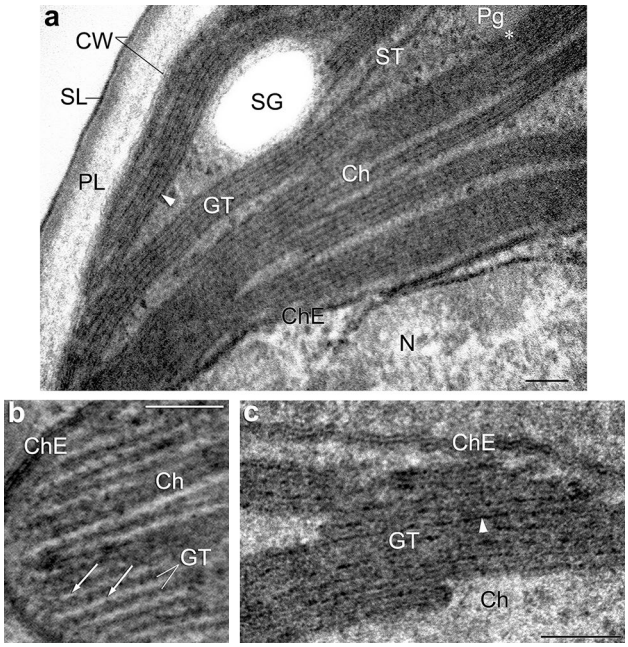

Fig. 4 Ultrastructure of thylakoids in the chloroplasts of *Desmodesmus* sp. 3Dp86E-1 cells grown in complete medium. **a, c** Stromal and granal thylakoids with narrow lumen filled with an electron-dense matter (7 and 9 days, respectively). **b** Transient expansion of the thylakoids (2nd day). *GT* granal thylakoids, *ST* stromal thylakoids; for other designations, see legend to Fig. 2. *Asterisk* indicates the contact between a plastoglobuli and a thylakoids. *Arrows* point to the thylakoids with expanded lumen. *Arrowheads* point to the electron-dense matter filling the thylakoid lumen. *Scale bars* 0.1 μm

to the level of 0.65, whereas in the '−N' cells, Q_y declined till the end of cultivation. Interestingly, the drop in Q_y recorded in the '+N' cells at the 2nd day of cultivation was accompanied by the transient expansion of the thylakoids observed in ca. 20 % of the cells studied (Fig. 4b); this was not the case in the '−N' cells.

In the '+N' cells, the chloroplasts featured a well-developed granae-lamellar system composed predominantly by granal thylakoids (2–16 per stack) together with a lower number of stromal thylakoids. The stromal thylakoids were occasionally arranged in parallel, up to seven at a time. The thylakoid lumen was narrow (≤4–5 nm), usually filled with an electron-dense matter forming a continuous layer or distinct bodies (Figs. 4a, c). By the 17th day of cultivation, the proportion of cells with expanded thylakoids was increased considerably (to ca. 40 % of the population). The expanded thylakoids featured the lumen of irregular width (7–12 nm) lacking the electron-dense matter.

The '−N' cells were characterized by a gradual, more rapid in comparison with the '+N' cells expansion of the thylakoids. The general organization of the thylakoids typical of '+N' cells was retained till the 7 day of cultivation. The lumen of the '−N' cells was electron-transparent, initially 5–8 nm (occasionally 17 nm) wide, later expanding to 12–15 nm, often to 20–57 nm (Figs. 5a, b); the latter cases were designated as 'thylakoid swelling'. As a result, after 17 days of cultivation, approximately one-half of the '−N' cells possessed dramatically expanded (swollen) thylakoids. Some cells contained the chloroplast with large zones filled with fragmented thylakoids or lacking thylakoids at all (Fig. 5c).

The pyrenoid frequency declined in the course of cultivation. Thus, more than 59 % of the cells studied at the day 0 possessed a well-developed pyrenoid. The frequency of pyrenoid increased to 84 % in the '+N' cells during exponential growth phase (7th day) and declined to 45 % upon reaching the stationary phase. Unlike the '+N' cells, pyrenoid frequency declined steadily in the '−N' cells to ca. 17 %. At the same time, pyrenoid degradation was detected (Fig. 6a).

Changes in cytoplasmic and plastidial inclusions

In the '+N' cells, the number of SG increased significantly only after 7 days of cultivation. In the '−N' cells, the increase in SG took place after the second day but was followed by a decrease after 7 days of cultivation. As a result, the '−N' cells contained ca. two times lower number of SG than the '+N' cells by the 17th day of cultivation (Fig. 7).

In the '+N' cells, a moderate buildup of cytoplasmic OB was recorded by the 9th day of cultivation. Most (75–90 %) of the investigated cells contained 12 times higher number OB that was recorded at the time 0; at the same time, the average OB diameter increased in the '+N' cells only 2.4 times (Figs. 2b, 8). These changes in the OB size and number were accompanied by ca. three-time increase in total fatty acid content (Fig. 8).

In the N-starving cells, a remarkable buildup of OB took place (Fig. 8). This buildup was apparent after the first

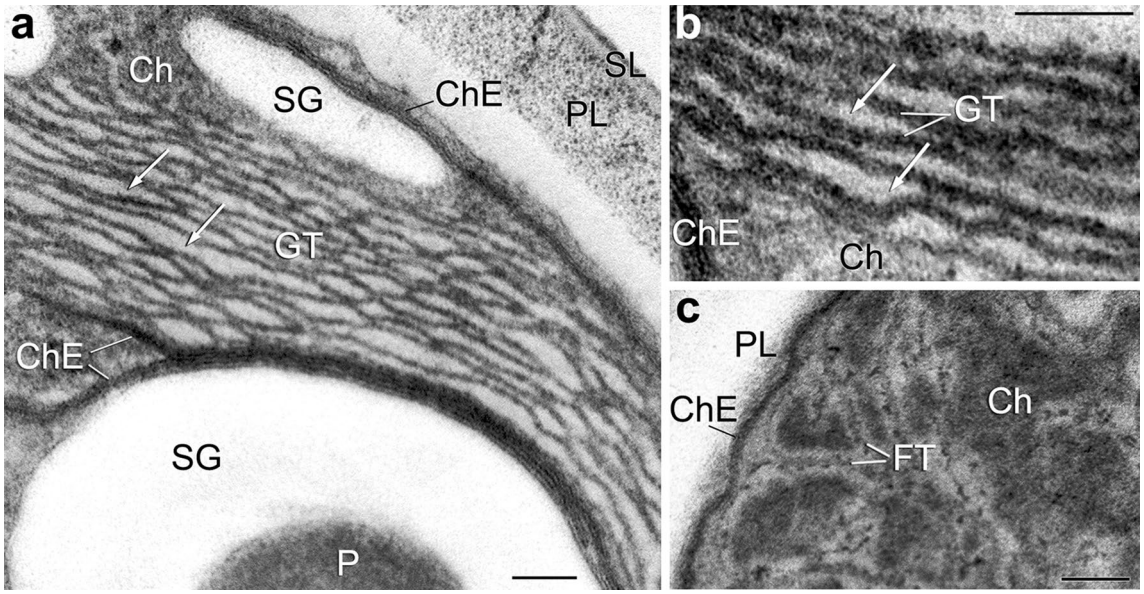

Fig. 5 Ultrastructure of thylakoids in the chloroplasts of *Desmodesmus* sp. 3Dp86E-1 cells grown in N-free medium. **a**, **b** Swelling of thylakoids (9th day). **c** Thylakoid fragmentation and thylakoid-lacking zones. *FT* fragmented thylakoids; for other designations, see legends to Figs. 2 and 4. *Arrows* point to the swollen thylakoids. *Scale bars* 0.1 μm

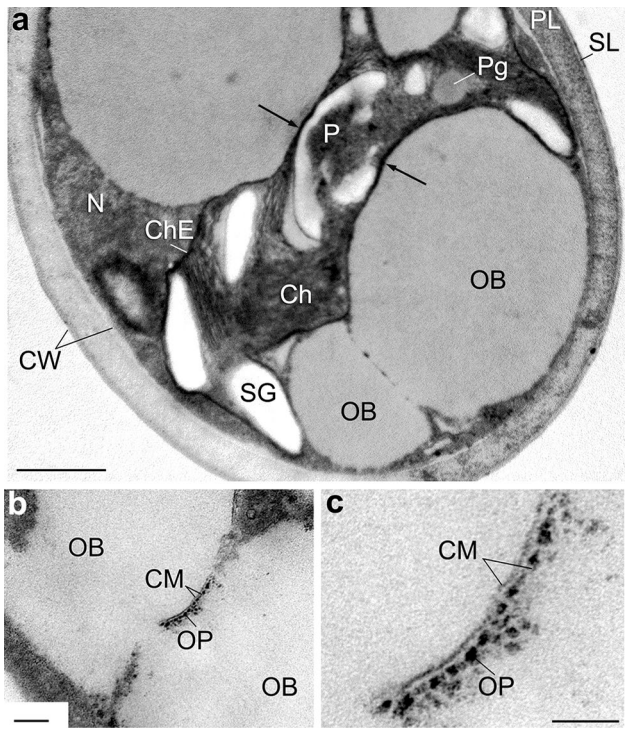

Fig. 6 Ultrastructure of *Desmodesmus* sp. 3Dp86E-1 cells grown on N-free medium for 9 days. **a** General view of the cell. **b** The region of fused oil body contact. **c** A close-up on the combined monolayer of the fused OB shown in **b** *CM* combined monolayers; for other designations, see legends to Figs. 2 and 4. *Arrows* point to the contacts between chloroplast envelope and OB. *Scale bars* **a** 0.5 μm, **b** 0.1 μm, **c** 0.05 μm

2 days of cultivation: in the inoculum cells, OB frequency was 20 %; after 2 days of N starvation, OB were encountered in 80 % of the cell population, and after 7 days, each N starvation contained OB (Figs. 2c, 6). As a result, the proportion of OB in the total area of the protoplast increased four times; the number and diameter of the OB in the '−N' cells were twice higher than in the '+N' cells, and total fatty acid content in the cells increased nearly ninefold (Fig. 8).

The ultrastructure of OB was similar in '+N' and '−N' cells. The OB were characterized by low or medium electron density, often with fine-grained osmiophilic depositions or globules (100–170 nm in diameter) at the periphery. In many cases, OB were revealed closely contacting with chloroplast envelope (Figs. 2b, c, 6a). At advanced stages of N starvations, large OB tended to fuse. Closely appressed fragments of the polar lipid monolayers surrounding the fused OB often remained in the region of their contact (Fig. 6). The combined thickness of two monolayers was 7–9 nm. Osmiophilic particles were often embedded in the monolayers (Fig. 6c).

In all cells studied, plastoglobuli (Pg) were revealed in the stroma of the chloroplast (Figs. 2, 4), as a rule in contact with the thylakoid membranes. Electron-dense Pg were normally present in the cells of the initial culture (day 0), whereas by the end of cultivation, Pg of medium and low electron density were more frequent. The size and number of Pg did not change significantly in the '+N' cells. Although N starvation lead, after 17 days of cultivation,

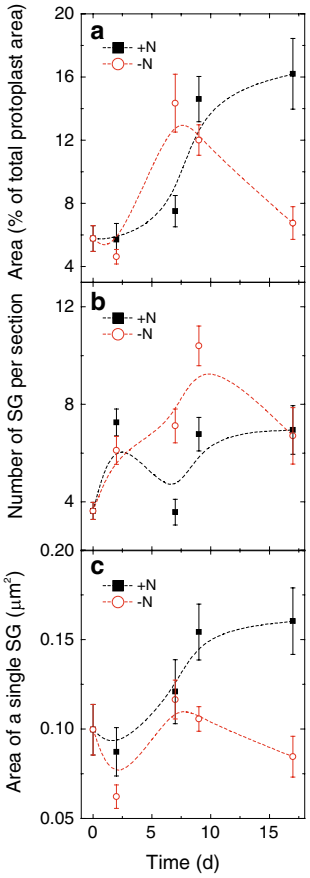

Fig. 7 Dynamics of the SG in the *Desmodesmus* sp. 3Dp86E-1 cells grown in complete (*closed symbols*) or (*open symbols*) N-free medium. **a** Proportion of the SG area in the total protoplast area. **b** SG number per cell section. **c** Mean area of a single SG

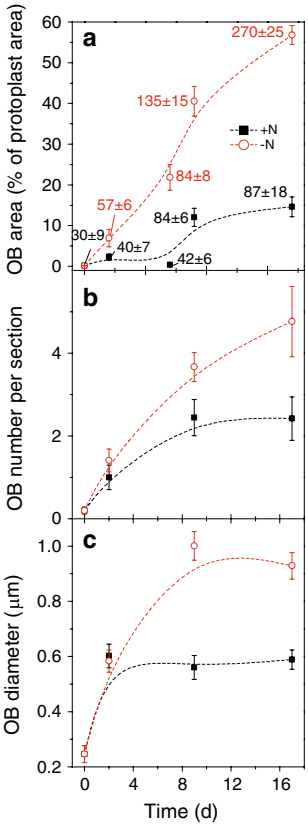

Fig. 8 Dynamics of the OB in the *Desmodesmus* sp. 3Dp86E-1 cells grown in complete (*closed symbols*) or (*open symbols*) N-free medium. **a** Proportion of the OB area in the total protoplast area. **b** OB number per cell section. **c** Mean OB diameter. Numbers in **a** denote total fatty acid content in the biomass (mg/g DW)

to ca. five-time increase in total Pg volume in comparison with the '+N' cells, the absolute volume of Pg was several orders of magnitude lower in comparison with that of OB (Table 1).

Changes in the cell wall

All cells studied featured the similar CW structure comprised by the inner polysaccharide layer and the external trilaminar sporopollenin layer (Figs. 2, 4–6). The latter layer formed diverse epistructures, described in more detail by Gorelova et al. (2012), which were retained under N starvation.

Average CW thickness value is the characteristic of a heterogeneous population comprised by cells of different ages. The average CW thickness of the newly divided *Desmodesmus* sp. cells was 0.057 ± 0.002 μm, increased to 0.220 μm in mature N-sufficient cells. The CW of the '+N' cells occupied 8–11 % of the cell section area. The CW thickness of the rapidly dividing cells in the middle of the exponential phase (7th day) was ca. 30 % lower than in the stationary phase culture comprised mainly by nondividing cells (Fig. 9a).

By contrast, the CW thickness of the '−N' cells increases nearly three times during 9 days of cultivation and became, by the end of the experiment (by the 17th day), approximately 58 % thicker as compared to the CW of the '+N' cells (Fig. 9b). The thickness of the sporopollenin layer did not change significantly regardless of N availability and the duration of cultivation, whereas the thickness of the polysaccharide layer increased remarkably so the polysaccharide layer made the main contribution to the overall increase in the CW in the '−N' cells which was 2.5 times thicker than in the '+N' cells (Fig. 9).

Correlation between the parameters of photosynthetic and storage compartments

Chloroplast is both photoassimilatory and storage cell compartment where the excessive photosynthates are deposited (mainly in the form of SG). The major extraplastidic storage

Table 1 Plastoglobuli in the cells of *Desmodesmus* sp. 3Dp86E-1 grown in the complete or N-free medium

Parameter	N availability			
	+N		−N	
Cultivation time, days	7	17	7	17
Frequency (% of the cells studied)	80	84	70	76
Average number per section	3.04 ± 0.46	2.00 ± 0.48	1.90 ± 0.40	1.67 ± 0.23
Average diameter, μm	0.121 ± 0.006	0.114 ± 0.006	0.175 ± 0.005	0.203 ± 0.007
Total volume, $\times 10^{-4}$ μm^3	28.5	15.4	53.6	73.2

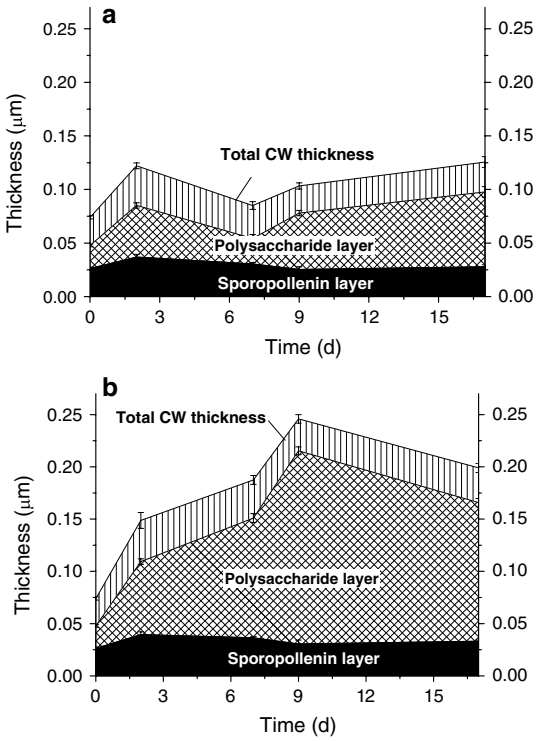

Fig. 9 Changes in the thickness of CW and its polysaccharide and sporopollenin layers of the *Desmodesmus* sp. 3Dp86E-1 cells grown in **a** complete or **b** N-free medium

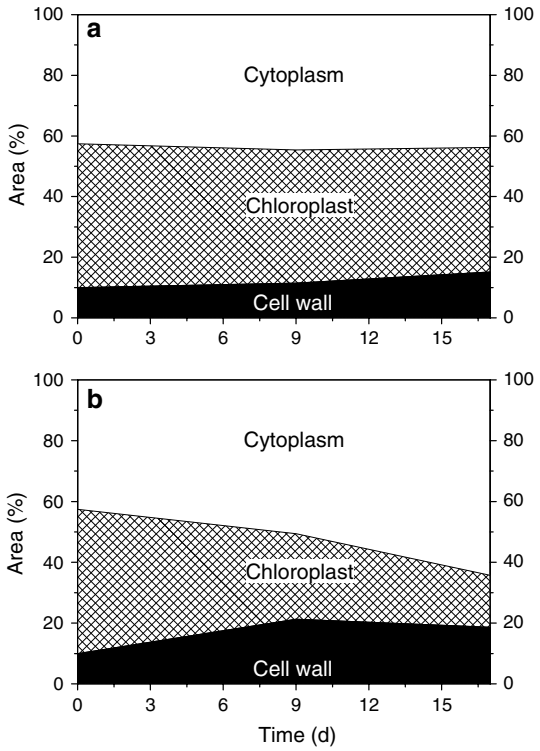

Fig. 10 Changes in the proportions of cytoplasm, chloroplast, and CW within the area of the *Desmodesmus* sp. 3Dp86E-1 cells grown in **a** complete or **b** N-free medium. Average values are shown; SE <5 % of the corresponding average

subcompartment is comprised by OB (Figs. 2, 6, 8). As could be seen from Figs. 9b and 10, CW is another compartment capable of accumulating significant photosynthate amounts in the *Desmodesmus* sp. In the '+N' cells, the ratio of major cell compartments such as chloroplast, CW, and cytoplasm (estimated as the protoplast excluding the chloroplast) was relatively stable in the course of cultivation. By contrast, in the '−N' cells, conspicuous changes were recorded in the ratio of the major compartments (Fig. 10).

The comparative analysis of the ultrastructural data revealed characteristic relationships between morphometric parameters of different compartments (Fig. 11). Thus, relative OB area displayed strong ($r^2 > 0.95$) negative relationship with relative chloroplast area (Fig. 11a). Notably, these relationships for the '+N' and '−N' cells followed a similar trend. Oil body size also exhibited a tight ($r^2 > 0.9$), slightly nonlinear relationships with the polysaccharide layer thickness of the CW regardless of N presence in the cultivation medium; by contrast, no relationship was found between OB diameter and the thickness of sporopollenin layer (*cf.* squares and stars in Fig. 11b).

Discussion

Mechanisms underlying the stress-induced alterations of the photosynthate allocation, including the resulting

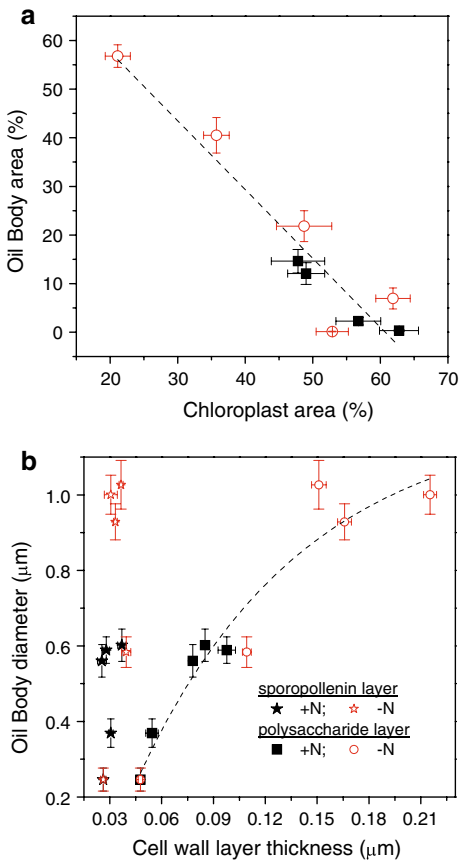

Fig. 11 **a** Relationships between the proportions of OB and chloroplast in the protoplast area and **b** relationships between the thickness of different layers of the CW and oil body diameter in the *Desmodesmus* sp. 3Dp86E-1 cells grown in complete (*closed symbols*) or (*open symbols*) N-free medium. *Asterisks*: sporopollenin layer. *Squares*: polysaccharide layer

ultrastructural changes, are relatively well studied in different taxa of free-living microalgae (Přibyl et al. 2013; Simionato et al. 2013; Yang et al. 2013), whereas the reports on symbiotic species, especially concerning representatives of Chlorophyta, are much scarcer. To bridge, at least in part, this gap, we focused on the effect of combined high light- and N-starvation stresses on the cell ultrastructure of a symbiotic chlorophyte from a marine benthic invertebrate.

The combination HL−N stress but not HL alone changes the C/N ratio of the cell

Under our experimental conditions, cultivation on N-replete medium under HL conditions does not trigger a sizable change in C/N ratio, which remained at the level of ca. 5 (Fig. 1) and was similar to the C/N characteristic of marine free-living (Lourenço et al. 1998) and symbiotic zooxanthellae (*Symbiodinium* sp. Freudenthal, Dinophyceae) of sea anemones (Muller-Parker et al. 1996). The transient peak of N content observed in our experiment is in agreement with the reports stating that the maximum rate of N absorption by microalgae from the medium is recorded in the first 1–3 days of cultivation (Cunningham and Maas 1978; Li et al. 2011).

The relatively stable C/N ratio suggests the relatively small flux of the excessively fixed carbon in the '+N' cells where the bulk of photosynthates is evidently utilized for the multiplication of the cells. By contrast, the combination of HL and N starvation brought about a considerable increase in C/N (from 5 to 16 by the 7th day), which could be a manifestation of significantly higher flux of the excessively fixed carbon in the cells subjected to the combined stress.

The mode of HL response of the photosynthetic apparatus depends on N availability

Similarly to free-living chlorophytes (Merzlyak et al. 2007; Solovchenko et al. 2010, 2013b), the symbiotic *Desmodesmus* sp. responded to HL by a swift decline in chl content and photosynthetic activity at a rate which was, for the first 2 days of observation, independent of N availability (Fig. 1b). Later, chl content leveled off in the '+N' cells but in the '−N' cells the decline went on, so did the photosynthetic activity. This process, as evidenced by fatty acid composition changes, presumably was accompanied by the loss of membrane lipids (Fig. 8; Table 2). These results are in line with HL-induced accumulation of storage lipids on the background of the membrane lipid decomposition previously found in this microalga (Solovchenko et al. 2013a).

Table 2 Typical changes in the lipid fatty acid composition of the *Desmodesmus* sp. 3Dp86E-1 cells grown at 480 μmol PAR photons m^{-2} s^{-1} in complete or N-free medium for nine days

Fatty acid	% Of total fatty acids		
	0 days	9 days; +N	9 days; −N
Palmitic (16:0)	17.47	19.57	22.59
Palmitoleic (Δ7–16:1)	3.76	6.02	3.77
Hexadecatrienoic (Δ7, 10, 13–16:3)	3.75	4.34	3.73
Stearic (18:0)	4.16	2.77	2.37
Oleic (Δ9–18:1)	**27.52**	**40.34**	**39.49**
Linoleic (Δ9, 12–18:2)	15.08	14.53	16.89
α-Linolenic (Δ9, 12, 15–18:3)	**21.57**	**7.27**	**6.79**
Eicosanoic (20:0)	3.14	2.95	2.12
Eicosenoic (Δ11–20:1)	3.54	2.21	2.25
18:1/18:3 ratio	1.28	5.55	5.82
Unsaturation Index	129.70	99.43	99.66

The FA percentages exhibiting the most significant changes under the stresses are in bold

The changes in the thylakoid organization recorded in the *Desmodesmus* cells (Figs. 4, 5) could manifest different responses to HL exercised by cells depending on N availability in the medium. At the ultrastructural level, the stress effects on photosynthetic apparatus of the *Desmodesmus* sp. were apparent as (1) a decrease in the proportion of the STM in the total area of the protoplast at a rate similar to that of the decline in chl (Figs. 1b, 3) and (2) a decrease in the thylakoids packing density per unit STM area. The latter effect was due to the lumen expansion and appearance of large regions of the stroma devoid of granae thylakoids (Fig. 5a, b), a remarkable dismantling of the thylakoid membranes (Fig. 5c), and the increase in Pg size (Table 1).

Interestingly, the transient lumen expansion (the 2nd day of cultivation) occurred in the '+N' cells with the kinetics similar to that of the decline in Q_y. Possible reasons of the thylakoid expansion could be related with an overreduction of photosynthetic electron transport chain in the thylakoid membrane(s). Generally, such circumstances arise when the amount of the absorbed light energy is significantly higher than the sink capacity of the dark reactions, which is often the case under stress. As a result, various regulatory and photoprotective mechanisms such as phosphorylation and migration of outer light-harvesting antenna from photosystem II toward photosystem I are triggered. This process could be among the causes of the characteristic changes in thylakoid membrane topology (lumen expansion) under HL (Nagy et al. 2014). Notably, the transient simultaneous thylakoid expansion and Q_y decline occurred only in the '+N' cells and coincided with the maximum N content in the biomass (Fig. 1a). This circumstance suggests a possible contribution of reduced N forms such as ammonia to the partial photoinhibition observed at the 2nd day in the '+N' cells (Topf et al. 1992). Restoration of the lumen width was accompanied by the recovery of Q_{y-} which is compatible with our suggestion of a relationship between operation of photoprotective mechanisms in and the transient expansion of the thylakoids in the cells of microalgae.

Unlike the N-sufficient cells, the '−N' cells exhibited a sustained and considerably more rapid expansion of the thylakoid lumen increase resulting, in a significant proportion of the cell population, in thylakoid swelling (Figs. 4, 5). Remarkably, the extensive swelling of thylakoids in different oxygenic photosynthetic organisms (cyanobacteria, microalgae, higher plants) could be linked to a severe impairment of the electron transport in the thylakoid membranes (Barbato et al. 1992; Topf et al. 1992; Majeran et al. 2001; Johnson et al. 2011; Baulina 2012). Our observations of the lumen expansion and the thylakoid swelling are in agreement with the recorded decline in photosynthetic efficiency. In this case, it was difficult to discern the contributions of the photoacclimation and photoinhibition both leading to the overall reduction of the fixed carbon flux into the cell. Although the reduction of chloroplast is a well-known response of microalgae to N starvation described, e.g., in *Nannochloropsis oceanica* Suda et Miyashita IMET1 (Dong et al. 2013), *N. gaditana* Suda et Miyashita (Simionato et al. 2013), *Phaeodactylum tricornutum* Bohlin (Yang et al. 2013), *Galdieria sulphuraria* Merola (Sinetova et al. 2006), *Parietochloris incisa* S. Watanabe et G.L. Floyd (Merzlyak et al. 2007), it was not accompanied in these instances by thylakoid swelling. The *Chlamydomonas reinhardtii* Dangeard P.A. sta6 starchless mutant (Goodson et al. 2011) also did not display thylakoid swelling, although the micrographs presented in this work are evident of lumen expansion to 20–25 nm at the 4th day of N starvation. Furthermore, the loss of chl and phycobiliproteins in *Cryptomonas maculata* Marine Biol. Laboratory Plymouth, Culture 29 (Cryptophycophyta) was accompanied by uneven expansion of the lumen and deterioration of the thylakoid membranes (Rhiel et al. 1985). Symbiotic microalgae such as zooxanthellae of the coral *Pocillopora damicornis* Linnaeus responded to N starvation by a decline in the surface density of thylakoids but retained the size of the chloroplast (Berner and Izhaki 1994). On the other hand, starvation of sea anemone *Aiptasia pallida* Agassiz in Verrill caused the shrinkage of chloroplast of the symbiotic zooxanthellae (*Symbiodinium* sp.) but the surface density of thylakoids remained essentially the same (Muller-Parker et al. 1996).

In higher plants, stresses such as HL and N starvation promoting decomposition of thylakoid membranes often lead to the increase in size and number of Pg (Besagni and Kessler 2013) and, furthermore, to the formation of Pg clusters in chloroplasts (Austin et al. 2006). In the plastids of the N-starving starchless mutant *C. reinhardtii* sta6, large lipid droplets, probably developing from Pg, were found (Goodson et al. 2011). In the microalga under investigation, the combined action HL- and N-starvation stress lead to an increase in Pg size, and at the same time, the number of Pg did not change significantly. Probably, this was the case since HL, especially in N-starving cells, is conductive for the biosynthesis of reserve but not membranal lipids so there might be a decline in the amount of glycolipids (as well as proteins) necessary for the formation of new Pg (Besagni and Kessler 2013). By contrast, TAG accumulated under these conditions could be deposited in these structures promoting the expansion of existing Pg.

Similarly, the extensive degradation of chloroplast membranes in N-starving diatom *P. tricornutum* at late exponential was accompanied by a decrease in Pg number, presumably due to the downregulation of the gene(s) encoding proteins associated with the Pg (Yang et al. 2013). Regardless of the stress intensity, it is unlikely that the Pg subcompartment accommodates a considerable part of the excessively fixed carbon in the *Desmodesmus*

sp. due to its relatively small size in comparison with cytoplasmic OB. The lower electron density of the Pg recorded in this microalga under the stress is evident of the decrease in the unsaturation of lipids comprising these structures since their osmiophilicity (the ability to react with OsO_4 during postfixation of the samples) correlates directly with the number of double bonds in the carbon backbone (Geyer 1973). This is in accordance with the decrease in the proportion of polyunsaturated fatty acids in this microalga (Table 2, see also Solovchenko et al. 2013a).

A remarkable reduction in the plastidial compartment in the '−N' cells suggests that this compartment could serve as a nitrogen pool supporting the cell division for the first several cycles after N deprivation (García-Ferris et al. 1996). In particular, the excess of RUBISCO located in the pyrenoid could be metabolized first. Thus, in photoheterotrophic *Euglena gracilis* Ehrenberg subjected to N deprivation, the abundant RUBISCO was rapidly and selectively degraded (García-Ferris and Moreno 1994); in *C. reinhardtii* CC-125 under strictly photoautotrophic conditions, immunoblot assays also indicated a pronounced reduction, triggered by N shortage, in large subunit of RUBISCO (Msanne et al. 2012). Since the bulk of RUBISCO is associated with the pyrenoid (McKay et al. 1991), one may speculate that similar processes, as evidenced by a steady decline in pyrenoid frequency, could take place in the *Desmosmus* sp., under investigation. Once the expendable RUBISCO pool is exhausted, decomposition of the ribosomes, photosynthetic pigment–protein complexes, and other soluble and membrane-bound proteins may follow under long-term N starvation on the background of the upregulation of the proteins participating nitrogen scavenging and protein recycling (García-Ferris et al. 1996; Abe et al. 2004; Wang et al. 2009; Hockin et al. 2012; Msanne et al. 2012; Dong et al. 2013).

On the background of the overall reduction of chloroplast, ca. 2.5-fold increase in the perimeter-to-area ratio of this organelle took place in the '−N' cells. This finding is compatible with the suggestion of the formation of additional sink for the excessive photosynthates by the elevated biosynthesis of the lipid building blocks of the chloroplast envelope. Furthermore, chloroplast envelope is evidently involved in biosynthesis and packaging of the cytoplasmic OB (Goodson et al. 2011; Li et al. 2012). Moreover, in *C. reinhardtii,* TAG are assembled from DAG made by chloroplast-specific acyltransferases and the chloroplast envelope membranes may be the sites of OB biogenesis (Fan et al. 2011; Nguyen et al. 2011; Li et al. 2012). Similar pathway of OB formation may operate in the *Desmodesmus* sp. studied in the present work since intimate contacts between OB and chloroplast envelope were often revealed (Figs. 2b, c, 6a).

SG and OB storage subcompartments are engaged sequentially under combined stress (whereas SG is sufficient under '+N' conditions)

A significantly different dynamics of the plastidial (SG) and cytoplasmic (OB) storage subcompartments was the characteristic of the '+N' and '−N' cells of *Desmodesmus* sp. (Figs. 7, 8a). A considerable part of the carbon fixed during first 7–9 days of cultivation under HL was allocated to starch biosynthesis regardless of N availability. Interestingly, as N starvation progressed, SG declined almost to the initial level, whereas OB expanded dramatically and occupied more than a half of cell volume. This latter process was accompanied by a considerable buildup of reserve lipids in the cell of the microalga (Fig. 8). At advanced stages of cultivation, there was a detectable increase in OB under the '+N' condition as well (Fig. 8a). The '+N' cultures did not encounter N limitation, and light limitation is also unlikely due to high illumination intensity and vigorous mixing of the culture. Taking into account these circumstances, the increase in OB at the stationary phase could be a consequence of a decline in the culture growth rate occurring on the background of high photosynthetic activity (see Fv/Fm values in Fig. 1b) generating under HL an increased flux of fixed carbon that is redirected to the storage compartment. It is difficult to pinpoint the exact reason of the slowdown of culture growth in this case, which in the batch culture could be related, e.g., with autoinhibition. It should be noted in addition that the induction of reserve compound synthesis under HL was also recorded in other microalgae even in the absence of nutrient limitation (Khozin-Goldberg et al. 2013).

Accordingly, the relationships between the storage subcompartments followed different trends in the '+N' and '−N' cells. Since the SG subcompartment is obviously unable to accommodate large amount of the excess carbon under N starvation, a considerable amount of it is allocated to OB from the beginning of N starvation (Fig. 8a) and the photosynthate flux was redirected from SG to OB, probably through de novo fatty acid biosynthesis (Khozin-Goldberg et al. 2013). Essentially, OB harboring neutral lipids with ca. twice higher energy storing capacity than starch (Subramanian et al. 2013) became the primary storage compartment providing the efficient sink under N starvation. The suggestion of TAG as main storage lipid in *Desmodesmus* sp. as well as the involvement of de novo fatty acid biosynthesis is supported by the increase in the proportion of saturated and monounsaturated fatty acids (mainly oleate, 18:1) recorded in our previous work on this microalga (Solovchenko et al. 2013a; see also Table 2).

Certain amount of SG is normally encountered in the plastids of microalgae even under favorable conditions (Goncalves et al. 2013). The initial rise in starch under

stress could be attributed to channeling of photosynthates to the most accessible storage compartment such as plastidial SG. It is known that in certain situations, such as blocking of the starch biosynthesis, e.g., in starchless mutants of *C. reinhardtii,* the excessive carbon is redirected to Pg and OB (Goodson et al. 2011). It was speculated that, under N starvation, the accumulation of TAG could involve pathways and substrates normally (under N-replete conditions) used for starch biosynthesis such as newly (photosynthetically) assimilated carbon. This could be a mechanism underlying the vast increase in OB at the expense of SG in the N-starving cells of *Desmodesmus* sp. recorded in this work. Interestingly, in *C. reinhardtii* CC-125 and *Coccomyxa* sp. Schmidle C-169 under strictly photoautotrophic conditions, nitrogen depletion triggered a similar pattern of early synthesis of starch followed by significant TAGs accumulation (Msanne et al. 2012). Similarly, the study of the transient accumulation of starch accompanied by gradual accumulation of neutral lipid in N-starving cells of *Pseudochlorococcum* P.A. Archibald grown under HL demonstrated that the starch and neutral lipids could be interconvertible (Li et al. 2011). In this case, partial inhibition of starch synthesis and degradation enzymes (ADP-glucose pyrophosphorylase and α-amylase) resulted in a decrease in neutral lipid content, indicating that conversion of starch to neutral lipid may contribute to overall neutral lipid accumulation. The possibility of the conversion of carbon from previously accumulated carbohydrate chrysolaminarin into lipids under silicon deficiency was demonstrated for the diatom *Cyclotella cryptica* Reimann, Lewin and Guillard (Roessler 1988). By contrast, a symbiotic zooxanthella of a coral responds to N deficiency by roughly equal increase in SG and OB (Berner and Izhaki 1994). At the same time, starvation of a sea anemone harboring *Symbiodinium* sp. causes only an increase in OB in the cells of the photobiont exerting no effect on starch (Muller-Parker et al. 1996). In addition, the changes in the SG and OB subcompartments could be related with carbohydrate and lipid catabolism proceeding at different rates as well as with respiratory effects, especially in the cells with impaired photosynthetic activity.

We would like to note in addition that the studied *Desmodesmus* sp. is obviously able to directly channel the excessive photosynthates to the TAG biosynthesis, at least in the first 7 days of N starvation when the degradation of thylakoid membranes was not yet observed but the OB subcompartment was expanded 2.5 times faster than the SG subcompartment in the same cells (3.1 % vs. 1.2 % day^{-1} as calculated per unit area of the protoplast). At the same time, the rates of the expansion of OB and SG subcompartments in the '−N' cells during the first 7 days of N starvation were, respectively, 103 and 7 times higher than in the '+N' cells. It seems to be likely that, at more advanced stages of N starvation, the synthesis of TAG was augmented by the building blocks released during the dismantling of the thylakoid membranes as in the free-living *P. tricornutum* (Yang et al. 2013) or *E. gracilis* (García-Ferris et al. 1996).

The recent proteomic investigations showed that significant amount of proteins associated with the biogenesis of the OB subcompartment (the enzymes involved in deacylation/reacylation, sterol synthesis, lipid signaling, and lipid trafficking) is often present in the isolated OB preparations (Nguyen et al. 2011). One may speculate that the fine-grained osmiophilic depositions or globules observed at the OB periphery and osmiophilic transmonolayer particles (Figs. 2b, c, 6) could be formed by such proteins. As evidenced by immunostaining electron microscopy, another plausible source of these depositions is a lipid droplet-stabilizing protein such as major lipid droplet protein (MLDP) associated with TAG-containing OB in the N-deprived *Dunaliella salina* Teodoresco (Davidi et al. 2012).

Polysaccharides of the cell wall provide an additional sink in N-starving cells

The increase in the proportion of CW in the overall cell area (Fig. 10) had drawn our attention to this structure. As revealed by morphometric analysis, cultivation under HL in N-replete medium had no sizeable effect on the CW of the *Desmodesmus* sp. cells (Fig. 9a). By contrast, in the N-starving cells, CW thickness increased nearly three times by the 9th day of cultivation (Fig. 9b). The sporopollenin CW layer did not change significantly, whereas the thickness of the polysaccharide CW layer increased dramatically (more than fourfold), suggesting an important role of CW in the formation of sink for the excessive photosynthates accumulated under stress. Remarkably, the polysaccharide CW layer displayed a strong positive correlation with the diameter of OB, a key storage structure increasing under the stress; this was not the case for sporopollenin layer (Fig. 11b). It is also notable that the onset of SG decomposition in the '−N' almost coincided with the boost of the CW polysaccharide biosynthesis (Fig. 2). These findings are compatible with the fact that in certain microalgae, the excessive photosynthates could be channeled, apart from the reserve lipids and carbohydrates biosyntheses, to the formation and/or renovation of cell cover structures (Dubinsky and Berman-Frank 2001).

Conclusion

Collectively, the results obtained in this work demonstrate that different mechanisms work concertedly to

prevent photooxidative damage to the *Desmodesmus* sp. cells stressed by high irradiance and N starvation. Importantly, the stress-induced changes in the ultrastructure of the symbiotic *Desmodesmus* sp. 3Dp86E-1 generally resemble those characteristic of free-living microalgae but have specific traits as well. Cultivation under HL caused the reduction of chloroplast, controlled dismantling of the granae-lamellar system, and a profound decline in photosynthetic activity, which was partially recovered in the '+N' but not in '−N' cells. This decline was accompanied by a transient expansion of thylakoids obviously manifesting an adaptive response to HL lacking in N-starving cells. By contrast, a gradual expansion of the thylakoids, at a higher rate than in the '+N' cells, was observed in the '−N' cells eventually resulting in the thylakoid swelling.

Similarly to other free-living species, *Desmodesmus* sp. 3Dp86E-1 responded to the stresses by a remarkable increase in different storage compartments; the exact set of the compartments involved and the kinetics of their changes depended on N availability. We would like to emphasize that the reduction in photoassimilatory compartment and expansion of the key carbon sink compartments (OB and CW polysaccharide layer) occurred in a highly synchronous manner regardless of the nature of the stress albeit SG comprised the obvious exception. One may speculate that, by the 9th day of N starvation, the sink strength of SG became insufficient to accommodate the excessively fixed carbon. As a result, the photosynthate flux was redirected to (1) cytoplasmic OB leading to a dramatic expansion of the latter and (2) polysaccharide layer of the CW.

Given the pronounced downregulation of the photosynthetic apparatus, the apparently limited sink capacity of the SG in *Desmodesmus* sp. 3Dp86E-1 seems to be sufficient to accommodate a relatively low flux of the excessively fixed carbon arising under HL even in the absence of N limitation. The combination of HL and N starvation generates a considerably higher flux of fixed carbon as evidenced by the C/N ratio. To cope with the combined stress, the deep rearrangement of the metabolism takes place and additional sinks are formed resulting in the profound alteration of the cell ultrastructure. Further research is needed to elucidate the nature of the 'metabolic switch' channeling the excessive photosynthate to different sinks within the microalgal cell under stress.

Acknowledgments The electron microscopy part of the work was carried out at the User Facilities Center of M.V. Lomonosov Moscow State University.

References

Abe J, Kubo T, Takagi Y, Saito T, Miura K, Fukuzawa H, Matsuda Y (2004) The transcriptional program of synchronous gametogenesis in *Chlamydomonas reinhardtii*. Curr Genet 46:304–315. doi:10.1007/s00294-004-0526-4

Austin JR, Frost E, Vidi P-A, Kessler F, Staehelin LA (2006) Plastoglobules are lipoprotein subcompartments of the chloroplast that are permanently coupled to thylakoid membranes and contain biosynthetic enzymes. Plant Cell 18:1693–1703. doi:10.1105/tpc.105.039859

Barbato R, Friso G, Rigoni F, Dalla Vecchia F, Giacometti GM (1992) Structural changes and lateral redistribution of photosystem II during donor side photoinhibition of thylakoids. J Cell Biol 119:325–335

Baulina OI (2012) Ultrastructural plasticity of cyanobacteria. Springer, Berlin

Berner T, Izhaki I (1994) Effect of exogenous nitrogen levels on ultrastructure of zooxanthellae from the hermatypic coral *Pocillopora damicornis*. Pac Sci 48:254–262

Besagni C, Kessler F (2013) A mechanism implicating plastoglobules in thylakoid disassembly during senescence and nitrogen starvation. Planta 237:463–470. doi:10.1007/s00425-012-1813-9

Cunningham A, Maas P (1978) Time lag and nutrient storage effects in the transient growth response of *Chlamydomonas reinhardii* in nitrogen-limited batch and continuous culture. J Gen Microbiol 104:227–231. doi:10.1099/00221287-104-2-227

Davidi L, Katz A, Pick U (2012) Characterization of major lipid droplet proteins from *Dunaliella*. Planta 236:19–33. doi:10.1007/s00425-011-1585-7

de Morais MG, Costa JAV (2007) Biofixation of carbon dioxide by *Spirulina* sp. and *Scenedesmus obliquus* cultivated in a three-stage serial tubular photobioreactor. J Biotechnol 129:439–445. doi:10.1016/j.jbiotec.2007.01.009

Dong H-P, Williams E, Wang D-Z, Xie Z-X, Hsia R-C, Jenck A, Halden R, Li J, Chen F, Place AR (2013) Responses of *Nannochloropsis oceanica* IMET1 to long-term nitrogen starvation and recovery. Plant Physiol 162:1110–1126. doi:10.1104/pp.113.214320

Dubinsky Z, Berman-Frank I (2001) Uncoupling primary production from population growth in photosynthesizing organisms in aquatic ecosystems. Aquat Sci-Res Across Boundaries 63:4–17

Fan J, Andre C, Xu C (2011) A chloroplast pathway for the de novo biosynthesis of triacylglycerol in *Chlamydomonas reinhardtii*. FEBS Lett 585:1985–1991. doi:10.1016/j.febslet.2011.11.001

Fernandes B, Teixeira J, Dragone G, Vicente AA, Kawano S, Bišová K, Přibyl P, Zachleder V, Vítová M (2013) Relationship between starch and lipid accumulation induced by nutrient depletion and replenishment in the microalga *Parachlorella kessleri*. Bioresour Technol 144:268–274. doi:10.1016/j.biortech.2013.06.096

Fisher T, Berner T, Iluz D, Dubinsky Z (1998) The kinetics of the photoacclimation response of *Nannochloropsis* sp. (Eustigmatophyceae): a study of changes in ultrastructure and PSU density. J Phycol 34:818–824

Folch J, Lees M, Sloane-Stanley G (1957) A simple method for the isolation and purification of total lipids from animal tissues. J Biol Chem 226:497–509

García-Ferris C, Moreno J (1994) Oxidative modification and breakdown of ribulose-1, 5-bisphosphate carboxylase/oxygenase induced in *Euglena gracilis* by nitrogen starvation. Planta 193:208–215

García-Ferris C, de los Ríos A, Ascaso C, Moreno J (1996) Correlated biochemical and ultrastructural changes in nitrogen-starved *Euglena gracilis*. J Phycol 32:953–963. doi:10.1111/j.0022-3646.1996.00953.x

Geyer G (1973) Ultrahistochemie. Histochemische Arbeitsvorschriften für die Electronmikroskopie. Veb Gustav Fischer Verlag, Jena

Goncalves EC, Johnson JV, Rathinasabapathi B (2013) Conversion of membrane lipid acyl groups to triacylglycerol and formation of lipid bodies upon nitrogen starvation in biofuel green algae *Chlorella* UTEX29. Planta 238:895–906. doi:10.1007/s00425-013-1946-5

Goodson C, Roth R, Wang ZT, Goodenough U (2011) Structural correlates of cytoplasmic and chloroplast lipid body synthesis in *Chlamydomonas reinhardtii* and stimulation of lipid body production with acetate boost. Eukaryot Cell 10:1592–1606. doi:10.1128/EC.05242-11

Gorelova O, Kosevich I, Baulina O, Fedorenko T, Torshkhoeva A, Lobakova E (2009) Associations between the White Sea invertebrates and oxygen-evolving phototrophic microorganisms. Mosc Univ Biol Sci Bull 64:16–22

Gorelova O, Baulina O, Solovchenko A, Fedorenko T, Kravtsova T, Chivkunova O, Koksharova O, Lobakova E (2012) Green microalgae from associations with White Sea invertebrates. Microbiol (Mikrobiologiya) 81:505–507. doi:10.1134/S002626171204008X

Guschina IA, Harwood JL (2009) Algal lipids and effect of the environment on their biochemistry. In: Arts MT, Brett MT, Kainz MJ (eds) Lipids in aquatic ecosystems. Springer, Heidelberg, pp 1–24

Hockin NL, Mock T, Mulholland F, Kopriva S, Malin G (2012) The response of diatom central carbon metabolism to nitrogen starvation is different from that of green algae and higher plants. Plant Physiol 158:299–312. doi:10.1104/pp.111.184333

Hüner NP, Bode R, Dahal K, Hollis L, Rosso D, Krol M, Ivanov AG (2012). Chloroplast redox imbalance governs phenotypic plasticity: the "grand design of photosynthesis" revisited. Front Plant Sci 3: article 255. doi: 10.3389/fpls.2012.00255

Johnson MP, Brain AP, Ruban AV (2011) Changes in thylakoid membrane thickness associated with the reorganization of photosystem II light harvesting complexes during photoprotective energy dissipation. Plant Signal Behav 6:1386–1390. doi:10.4161/psb.6.9.16503

Kates M (1986) Techniques of lipidology: Isolation, analysis and identification of lipids. Elsevier, Amsterdam

Khozin-Goldberg I, Shrestha P, Cohen Z (2005) Mobilization of arachidonyl moieties from triacylglycerols into chloroplastic lipids following recovery from nitrogen starvation of the microalga *Parietochloris incisa*. Biochim Biophys Acta 1738:63–71. doi:10.1016/j.bbalip.2005.09.005

Khozin-Goldberg I, Solovchenko A, Pal D, Cohen Z, Boussiba S (2013) Omega-3 and omega-6 LC-PUFA from photosynthetic microalgae: studies on *Parietochloris incisa* and *Nannochloropsis* sp. In: Catala A (ed) Polyunsaturated fatty acids: sources, antioxidant properties and health benefits. Nova Science Publishers, Hauppauge, pp 1–22

Li Y, Han D, Sommerfeld M, Hu Q (2011) Photosynthetic carbon partitioning and lipid production in the oleaginous microalga Pseudochlorococcum sp. (Chlorophyceae) under nitrogen-limited conditions. Bioresour Technol 102:123–129. doi:10.1016/j.biortech.2010.06.036

Li X, Moellering ER, Liu B, Johnny C, Fedewa M, Sears BB, Kuo M-H, Benning C (2012) A galactoglycerolipid lipase is required for triacylglycerol accumulation and survival following nitrogen deprivation in *Chlamydomonas reinhardtii*. Plant Cell 24:4670–4686. doi:10.1105/tpc.112.105106

Lourenço SO, Barbarino E, Marquez UML, Aidar E (1998) Distribution of intracellular nitrogen in marine microalgae: basis for the calculation of specific nitrogen-to-protein conversion factors. J Phycol 34:798–811

Majeran W, Olive J, Drapier D, Vallon O, Wollman F-A (2001) The light sensitivity of ATP synthase mutants of *Chlamydomonas reinhardtii*. Plant Physiol 126:421–433. doi:10.1104/pp.126.1.421

Maxwell K, Johnson G (2000) Chlorophyll fluorescence-a practical guide. J Exp Bot 51:659–668. doi:10.1093/jexbot/51.345.659

McKay RML, Gibbs Sarah P, Vaughn KC (1991) RuBisCo activase is present in the pyrenoid of green algae. Protoplasma 162:38–45

Merzlyak M, Chivkunova O, Gorelova O, Reshetnikova I, Solovchenko A, Khozin-Goldberg I, Cohen Z (2007) Effect of nitrogen starvation on optical properties, pigments, and arachidonic acid content of the unicellular green alga *Parietochloris incisa* (Trebouxiophyceae, Chlorophyta). J Phycol 43:833–843. doi:10.1111/j.1529-8817.2007.00375.x

Msanne J, Xu D, Konda AR, Casas-Mollano JA, Awada T, Cahoon EB, Cerutti H (2012) Metabolic and gene expression changes triggered by nitrogen deprivation in the photoautotrophically grown microalgae *Chlamydomonas reinhardtii* and *Coccomyxa* sp. C-169. Phytochem 75:50–59. doi:10.1016/j.phytochem.2011.12.007

Muller-Parker G, Lee KW, Cook CB (1996) Changes in the ultrastructure of symbiotic zooxanthellae (*Symbiodinium* sp., Dinophyceae) in fed and starved sea anemones maintained under high and low light. J Phycol 32:987–994

Nagy G, Ünnep R, Zsiros O, Tokutsu R, Takizawa K, Porcar L, Moyet L, Petroutsos D, Garab G, Finazzi G (2014) Chloroplast remodeling during state transitions in *Chlamydomonas reinhardtii* as revealed by noninvasive techniques in vivo. PNAS 111:5042–5047. doi:10.1073/pnas.1322494111

Nguyen HM, Baudet M, Cuiné S, Adriano JM, Barthe D, Billon E, Bruley C, Beisson F, Peltier G, Ferro M (2011) Proteomic profiling of oil bodies isolated from the unicellular green microalga *Chlamydomonas reinhardtii*: with focus on proteins involved in lipid metabolism. Proteomics 11:4266–4273. doi:10.1002/pmic.201100114

Přibyl P, Cepák V, Zachleder V (2012) Production of lipids in 10 strains of *Chlorella* and *Parachlorella*, and enhanced lipid productivity in *Chlorella vulgaris*. Appl Microbiol Biotechnol 94:549–561. doi:10.1007/s00253-012-3915-5

Přibyl P, Cepák V, Zachleder V (2013) Production of lipids and formation and mobilization of lipid bodies in *Chlorella vulgaris*. J Appl Phycol 25:545–553. doi:10.1007/s10811-012-9889-y

Reynolds E (1963) The use of lead citrate at high pH as an electron-opaque stain in electron microscopy. J Cell Biol 17:208–212

Rhiel E, Mörschel E, Wehrmeyer W (1985) Correlation of pigment deprivation and ultrastructural organization of thylakoid membranes in *Cryptomonas maculata* following nutrient deficiency. Protoplasma 129:62–73

Rippka R, Deruelles J, Waterbury JB, Herdman M, Stanier RY (1979) Generic assignments, strain histories and properties of pure cultures of cyanobacteria. J Gen Microbiol 111:1–61. doi:10.1099/00221287-111-1-1

Roessler PG (1988) Effects of silicon deficiency on lipid composition and metabolism in the diatom *Cyclotella cryptica*. J Phycol 24:394–400. doi:10.1111/j.1529-8817.1988.tb04482.x

Simionato D, Block MA, La Rocca N, Jouhet J, Maréchal E, Finazzi G, Morosinotto T (2013) The response of *Nannochloropsis gaditana* to nitrogen starvation Includes *de novo* biosynthesis of triacylglycerols, a decrease of chloroplast galactolipids, and reorganization of the photosynthetic apparatus. Eukaryot Cell 12:665–676. doi:10.1128/EC.00363-12

Sinetova M, Markelova A, Los D (2006) The effect of nitrogen starvation on the ultrastructure and pigment composition of chloroplasts in the acidothermophilic microalga *Galdieria sulphuraria*. Russ J Plant Physiol 53:153–162. doi:10.1134/S1021443706020026

Skjånes K, Rebours C, Lindblad P (2013) Potential for green microalgae to produce hydrogen, pharmaceuticals and other high value products in a combined process. Crit Rev Biotechnol 33:172–215. doi:10.3109/07388551.2012.681625

Solovchenko A (2012) Physiological role of neutral lipid accumulation in eukaryotic microalgae under stresses. Russ J Plant Physiol 59:167–176. doi:10.1134/S1021443712020161

Solovchenko A, Khozin-Goldberg I, Cohen Z, Merzlyak M (2009) Carotenoid-to-chlorophyll ratio as a proxy for assay of total

fatty acids and arachidonic acid content in the green microalga *Parietochloris incisa*. J Appl Phycol 21:361–366. doi:10.1134/S1021443713030138

Solovchenko A, Merzlyak M, Khozin-Goldberg I, Cohen Z, Boussiba S (2010) Coordinated carotenoid and lipid syntheses induced in *Parietochloris incisa* (Chlorophyta, Trebouxiophyceae) mutant deficient in Δ5 desaturase by nitrogen starvation and high light. J Phycol 46:763–772. doi:10.1111/j.1529-8817.2010.00849.x

Solovchenko A, Khozin-Goldberg I, Recht L, Boussiba S (2011) Stress-induced changes in optical properties, pigment and fatty acid content of *Nannochloropsis* sp.: implications for non-destructive assay of total fatty acids. Mar Biotechnol 13:527–535. doi:10.1007/s10126-010-9323-x

Solovchenko A, Chivkunova O, Semenova L, Selyakh I, Shcherbakov P, Karpova E, Lobakova E (2013a) Stress-induced changes in pigment and fatty acid content in the microalga *Desmodesmus* sp.isolated from a White Sea hydroid. Russ J Plant Physiol 60:313–321

Solovchenko A, Solovchenko O, Khozin-Goldberg I, Didi-Cohen S, Pal D, Cohen Z, Boussiba S (2013b) Probing the effects of high-light stress on pigment and lipid metabolism in nitrogen-starving microalgae by measuring chlorophyll fluorescence transients: studies with a Δ5 desaturase mutant of *Parietochloris incisa* (Chlorophyta, Trebouxiophyceae). Algal Res 2:175–182. doi:10.1016/j.algal.2013.01.010

Subramanian S, Barry AN, Pieris S, Sayre RT (2013) Comparative energetics and kinetics of autotrophic lipid and starch metabolism in chlorophytic microalgae: implications for biomass and biofuel production. Biotechnol Biofuels 6: article 150. http://www.biotechnologyforbiofuels.com/content/6/1/1

Topf J, Gong H, Timberg R, Mets L, Ohad I (1992) Thylakoid membrane energization and swelling in photoinhibited *Chlamydomonas* cells is prevented in mutants unable to perform cyclic electron flow. Photosynth Res 32:59–69

Wang ZT, Ullrich N, Joo S, Waffenschmidt S, Goodenough U (2009) Algal lipid bodies: stress induction, purification, and biochemical characterization in wild-type and starchless *Chlamydomonas reinhardtii*. Eukaryot Cell 8:1856–1868. doi:10.1128/EC.00272-09

Wellburn A (1994) The spectral determination of chlorophyll *a* and chlorophyll *b*, as well as total carotenoids, using various solvents with spectrophotometers of different resolution. J Plant Physiol 144:307–313. doi:10.1016/S0176-1617(11)81192-2

Yang Z-K, Niu Y-F, Ma Y-H, Xue J, Zhang M-H, Yang W-D, Liu J-S, Lu S-H, Guan Y, Li H-Y (2013). Molecular and cellular mechanisms of neutral lipid accumulation in diatom following nitrogen deprivation. Biotechnol Biofuels 6: article 67. http://www.biotechnologyforbiofuels.com/content/6/1/6

Zachleder V, Brányiková I (2014) Starch overproduction by means of algae. In: Bajpai R, Prokop A, Zappi M (eds) Algal biorefineries. Springer, Dordrecht, pp 217–240